



**HAL**  
open science

## HARMONI at ELT: a virtual instrument to get ready for the real one

Aurélien Jarno, Laure Piqueras, Johan Richard, Arlette Pécontal

► **To cite this version:**

Aurélien Jarno, Laure Piqueras, Johan Richard, Arlette Pécontal. HARMONI at ELT: a virtual instrument to get ready for the real one. Modeling, Systems Engineering, and Project Management for Astronomy XI, Jun 2024, Yokohama, Japan. pp.85, 10.1117/12.3019002 . hal-04720691

**HAL Id: hal-04720691**

**<https://hal.science/hal-04720691v1>**

Submitted on 3 Oct 2024

**HAL** is a multi-disciplinary open access archive for the deposit and dissemination of scientific research documents, whether they are published or not. The documents may come from teaching and research institutions in France or abroad, or from public or private research centers.

L'archive ouverte pluridisciplinaire **HAL**, est destinée au dépôt et à la diffusion de documents scientifiques de niveau recherche, publiés ou non, émanant des établissements d'enseignement et de recherche français ou étrangers, des laboratoires publics ou privés.



Distributed under a Creative Commons Attribution 4.0 International License

# HARMONI at ELT: a virtual instrument to get ready for the real one

A. Jarno<sup>\*a</sup>, L. Piqueras<sup>a</sup>, J. Richard<sup>a</sup>, A. Pécontal<sup>a</sup>

<sup>a</sup>Univ Lyon, Univ Lyon1, Ens de Lyon, CNRS, Centre de Recherche Astrophysique de Lyon  
UMR5574, F-69230, Saint-Genis-Laval, France

## ABSTRACT

HARMONI is the first light visible and near-IR integral field spectrograph for the ELT. It covers a large spectral range from 470nm to 2450nm with resolving powers from 3300 to 18000 and spatial sampling from 60mas to 4mas. It can operate in two Adaptive Optics modes – SCAO (including a High Contrast capability) and LTAO – or with NOAO. The project is preparing for Final Design Reviews. From the perspective of data reduction, HARMONI introduces unique challenges due to its multiple adaptive optics modes, four spatial scales, eleven gratings, and two distinct NIR detector read-out modes. Capitalizing upon CRAL's experience in developing instrument simulators, this complexity prompted the development of the HARMONI Instrument Numerical Model (HINM). Built upon standard astrophysical Python frameworks, this software uses the Fourier optics concept to propagate a wavefront through the instrument, and leverages existing simulation tools for adaptive optics, sky and detector simulation. This enables the generation of synthetic detector read-outs for both calibration and science exposures. This paper highlights the crucial role played by the HINM simulator to develop the data reduction pipeline and elaborate instrument calibration procedures.

**Keywords:** ELT, HARMONI, integral field spectrography, science software, simulation, numerical model, digital twin

## 1. INTRODUCTION

### The HARMONI instrument

HARMONI is a near-IR integral field spectrograph for the European Extremely Large Telescope (ELT) [1]. It will use image slicers to provide spectra over a single contiguous field measuring 204×152 spatial pixels (spaxels) in size. Four spaxel scales of 60×30, 20×20, 10×10 and 4×4 mas give fields of view on the sky of respectively 9.1×6.1", 4.1×3.0", 2.1×1.5" and 0.84×0.63" with increasing spatial resolution. Eleven spectral resolution settings of 3500, 7000 and 17000 are provided in all spatial scales, covering the wavelength range (not simultaneous) of 0.46–2.45 micrometers. The instrument has four operational modes: NOAO (seeing-limited), LTAO (Laser Tomography Adaptive Optics), SCAO (Single Conjugate Adaptive Optics), and HCAO (High Contrast using pupil tracking and SCAO), which cover a wide range of scientific aims.

Light from the telescope is relayed to the instrument by a cooled relay system, minimizing additional thermal background, to an 'up-looking' focus, which allows a gravity invariant rotating instrument configuration. Calibration light can be fed into the instrument via a deployable calibration system positioned upstream of the relay. The bulk of the instrument optomechanics are housed in a single cryostat at ~130K. A pre-optics subsystem provides the four selectable spatial pixel scales, in addition to other beam conditioning functions such as filters and pupil masks. The rectangular pre-optics output field is rearranged into four linear slits by the Integral Field Unit (IFU) subsystem, each feeding one of four spectrograph subsystems. The spectrographs collimate, disperse, and focus the light onto detectors, providing a choice of spectral ranges and resolving powers. Each spectrograph has one camera for the near-infrared range (0.8–2.45 micrometers) and up-to one for the visible range (0.46–0.82 micrometers), each camera having a pair of 4k×4k detectors. The baseline funding only provides visible cameras in two of the four spectrographs.

The international consortium developing HARMONI is led by the University of Oxford and the UK-ATC in Edinburgh. Centre de Recherche Astrophysique de Lyon (CRAL) is responsible for the IFU and the Science Software, which includes the data reduction pipeline and the instrument numerical model. The project is preparing for Final Design Reviews (FDR).

## The need for a virtual instrument

As shown in the previous section, HARMONI is by design a complex instrument split into several key systems that shall be integrated with challenging and sometimes contradictory constraints. Each of these systems, built and validated by different institutes, is a collection of major components whose interaction determines the key performances of the instrument, such as image quality and sensitivity. In addition, HARMONI will offer astronomers a wide range of observing modes and configurations, making the development of the data reduction pipeline challenging. This led us to develop the HARMONI Instrument Numerical model (HINM) software, which generates synthetic detector read-outs for both calibration and science exposures. It is already used or will be used to:

- Check the instrument design and provide feedback during its development. The goal is to predict possible problems well in advance before they become difficult to correct, but also to provide inputs for performance-related trade-offs.
- Provide simulated raw data to develop the data reduction pipeline, and especially the prototypes of algorithms identified as critical, which have to be delivered for FDR.
- Provide inputs and support for the verification and calibration campaigns before on-sky data becomes available. In particular simulated data will be used for an early validation of the requirements before the on-sky commissioning.
- Provide inputs and support to prepare the future observations having a good knowledge of the instrument uncertainties, as it is essential to minimize tests on sky and to optimize the ELT time. As such it is complementary to the HSIM software [2] which provides a faster but simplified simulation of HARMONI observations.

## 2. HINM: THE DIGITAL TWIN OF HARMONI

### The HINM software overview

The HINM software is the digital twin of HARMONI from the optical point of view. It uses the Fourier optics concept to mimic the light path throughout the atmosphere, the telescope and the instrument. It is built upon standard astrophysical Python frameworks (NumPy, SciPy and Astropy), and leverages existing simulation tools for adaptive optics, sky and detector simulation.

To simulate an exposure, the software ingests as input a configuration file describing the instrument configuration and the environmental conditions, plus either the configuration of the calibration module or a user-provided astrophysical scene (data-cube). Since HARMONI is an integral field spectrograph, the representation of light in the input data is inherently wavelength dependent. Our software propagates it as monochromatic images, wavelength by wavelength, from image plane to image plane, through a virtual atmosphere, the virtual ELT with adaptive optics, through the virtual instrument up to the detectors, simulating optical aberrations, diffraction, throughput, and detectors effects. At the end of the simulation, it creates raw FITS files similar to the ones that will be provided by the final instrument.

### Propagating light through an instrument module

In our simulator, we define an instrument module as a set of optics that propagates monochromatic images from one image plane to another. This generally aligns with the way an instrument is divided into subsystems, as interfaces are easier to define at an image plane than at a random plane. This is the case for HARMONI, where the optical models we have defined correspond to the subsystems (see left column of Figure 1).

From the software perspective, we define an instrument module as an object that, for a given wavelength, is able to:

- Compute forward and backward coordinate transforms between the input and output planes of the module;
- Propagate images associated with a coordinate system including a sampling step and a center, from the input plane to the output plane of the module at a given wavelength;

- Apply a transmission curve to a vector representing a flux spectrum or a transmission curve as a function of wavelength.

We have defined various type of these instrument modules. The simplest, for instance, simulates a rotation and is used among other things to mimic the HARMONI cryostat rotation. Another instrument module simulates a mask wheel. There are also debugging modules able to print information or dump an image for diagnostic purposes.

### **Fourier optics instrument module**

The most advanced instrument module implemented is based on the concept of Fourier optics [3]. Assuming the far-field Fraunhofer diffraction regime, we compute the complex amplitude between conjugate planes (e.g., between the exit pupil plane and the exit image plane of an optical system), using a Fourier transform. This module considers a paraxial optical system, and requires an input image mask, the equivalent focal lengths, a pupil mask and a set of wavefront error maps. The instrument optical design is used to define the equivalent paraxial optical system. In this equivalent system, the wavefront error maps are chromatic and field-dependent, therefore the set of wavefront error maps needs to cover the wavelength range and the field of view of the instrument module with a regular sampling. The wavefront error maps are first interpolated to the wavelength at which the propagation is performed, and from there a grid of point spread functions (PSF) covering the field of view are computed.

Finally, the input image is convolved with the set of PSFs, using a shift-variant blur technique [4]. In addition, this instrument module models the coordinate transforms between the input and output planes with 3D polynomials, enabling fast computation using a few multiplications and additions. In turns those are used to model the geometric transformations of an image within an instrument module by first computing the non-regular output grid corresponding to a regular input grid, and then resampling the image onto a regular grid. The corresponding intensity modulation is computed by using the Jacobian determinant of the polynomial.

### **Atmosphere instrument module**

For ground-based instruments it is essential to consider the various atmospheric effects, at least the most important ones. Our goal is to simulate these effects in a manner that is both realistic and compatible with the resolution of the instrument, rather than modeling them with high precision. To achieve this, we leverage existing tools, when possible, wrapped into an instrument module.

Atmospheric turbulence is simulated coupled with the adaptive optics of the instrument. Currently the AO PSF are simulated by copying the corresponding code from HSIM, based on the original code developed by the HARMONI adaptive optics Team [5]. This code can compute PSF for various wavelength and positions within the field of view, based on parameters such as adaptive optics mode, turbulence, natural or laser guide start distance, etc. We are however working on replacing this code with TIPTOP [6], a Python library capable of quickly computing PSF for many kinds of adaptive optics systems. TIPTOP is set to become the de facto standard library for future VLT and ELT instruments, and it is also planned for use in exposure time calculators and PSF reconstruction pipelines, using the same models across all the tools.

The atmosphere also affects wavelength dependent transmission due to Rayleigh scattering by air molecules, Mie scattering by aerosols, and molecular/aerosol absorption, which varies with the pointing direction and atmospheric conditions. These effects are modeled using the ESO SkyCalc sky model [7] [8].

Finally, the atmosphere influences the apparent position of objects in the sky depending on the wavelength and airmass, Since the refractive index of air is somewhat larger than one, light coming from outside the Earth's atmosphere is refracted towards zenith. This effect is significant for instruments with a high spatial resolution such as HARMONI. We model this in the atmosphere instrument module using coordinate transforms derived from the Filippenko equations [9].

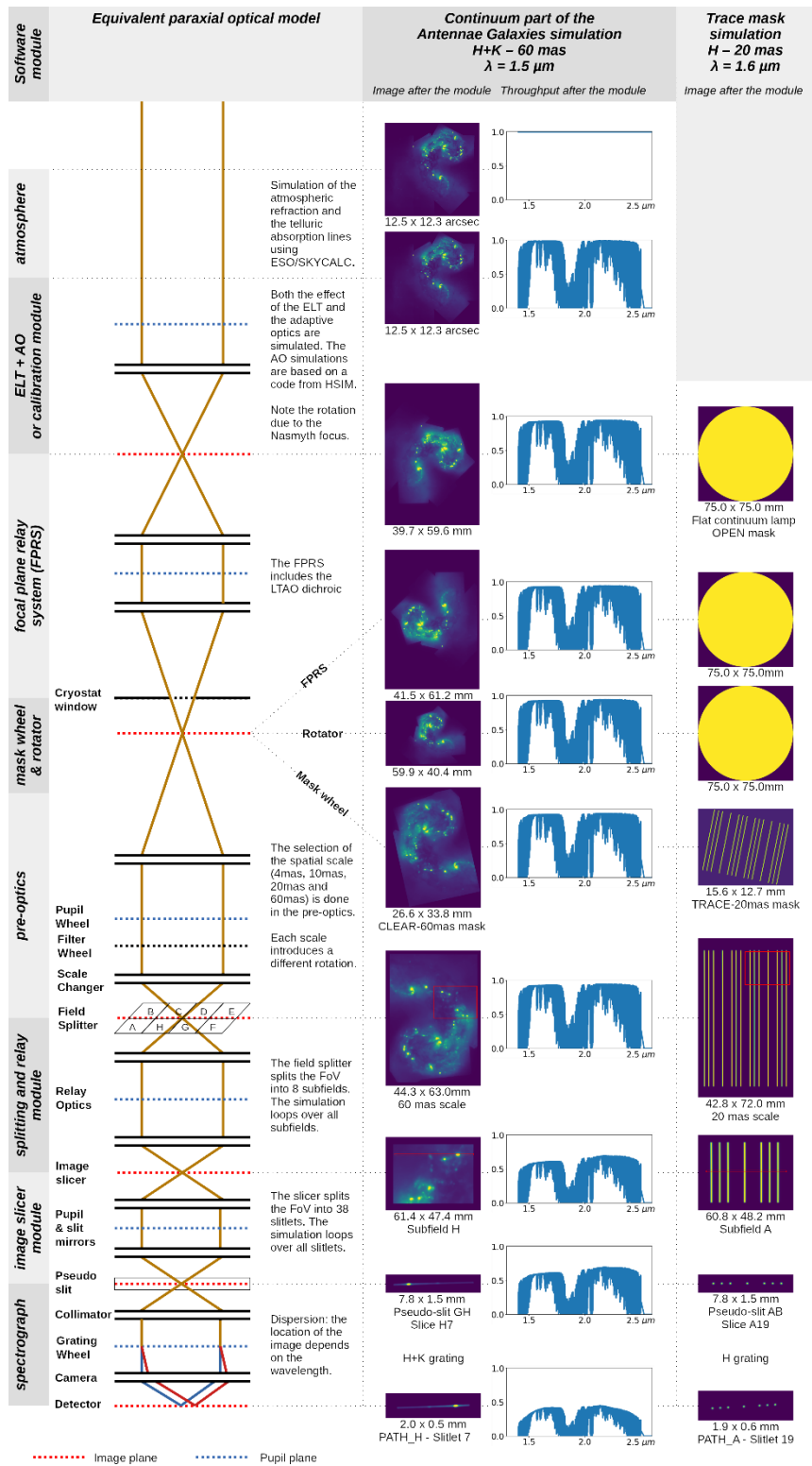


Figure 1. Equivalent paraxial model of the HARMONI instrument, and step by step example of propagation for the continuum part of the Antennae Galaxies and for a calibration mask. One can notice the effect of the atmosphere on the vector (here representing the transmission), the field rotation and the anamorphosis (for the 20 mas scale only) introduced by the pre-optics, as well as the slicing of the field of view first by the field splitter and then by the slicer.

## Propagating light through the instrument

The ability to model the propagation of an image through an instrument module is used to mimic the light propagation, by chaining them to model the sky, the ELT and the adaptive optics, and the various subsystems of the instrument up to the detectors. The inputs of a simulation are first translated into a product of a vector (flux spectrum or transmission curve as a function of wavelength) and a list of monochromatic images ordered by wavelength. The product represents a surface and spectral power density, expressed in  $W/m^3$ . This way flux conservation is maintained even if an image is resampled by the instrument module. The chosen number of images depends on the properties of the input data as for instance the spectral variation being smooth or sharp.

The list of images and the vector are then propagated through the chain of instrument modules up to the detectors, and for every optical path when optics split the field of view. Figure 1 illustrates this process step by step for a given slice and for two scenarios:

- The simulation of the continuum part of the Antennae Galaxies, using the LTAO mode, H+K grating and the 60 mas scale. This simulation starts from the object in the sky and the images are shown at a wavelength of 1.5 micrometers. Here the initial vector represents a transmission, as the spectrum is already contained in the list of images, and therefore begins with all one values. The list of images contains 40 evenly spaced monochromatic images over the grating wavelength range.
- The simulation of a trace mask in the pre-optics mask wheel, using the H grating and the 20 mas scale. The simulation starts at the level of the calibration module where the calibration lamps of the instrument are located. The spectrum of the continuum lamp being smooth spectrally, the list of image contains 10 evenly spaced monochromatic images over the grating wavelength range, while the vector contains the continuum lamp spectrum.

At each step the output image is computed from the input image, taking into account the point spread function and the geometric transformation introduced by the optics of the instrument module. In parallel the output vector is derived from the input vector, considering the transmission of the instrument module. In both cases resampling may be necessary to model the effects with sufficient precision. Some instrument modules have more than one successor, for example, to model each slice of the image slicer, in which case the propagation is performed by iterating over the successors. On Figure 1 one can notice, among other things, the effect of the atmosphere on the vector (here representing the transmission), the field rotation and the anamorphic magnification of a factor two (for the 20 mas scale only) introduced by the pre-optics, as well as the slicing of the field of view first in eight subfields by the field splitter (labeled A through H) and then into 38 slitlets by the image slicers. At the last step, the spectrograph modules disperse the light, and as we only consider monochromatic images, the dispersion only affects the center of the images.

The propagation through the chain of instrument modules results, at the detector level and per slice, in a list of images associated with a vector, representing for each wavelength the flux that reaches the detector. Therefore, for a given input covering the whole field of view, the full simulation results in 304 lists of images corresponding to the total number of slices in the instrument.

## Exposure simulation

Each image from a list will end up in a specific location on the detector, following the dispersion law. These data need to be interpolated in the wavelength direction in order to be summed on an oversampled detector map of a factor 3. For that we compute the centers of the corresponding slice on the detector plane as a function of wavelength, which provides us with the trace that the images will follow on the detector. Figure 2 shows this trace as a red line between three successive images on the left and a zoomed-in view of the trace to highlight the distortion effect on the right.

Then, we loop on the monochromatic images of the list, and we expand each image from its previous image to its next image along the dispersion direction (y in the figures), we convert its values to photon rates, and we finally add this resulting image on the detector grid. For that, for each image:

- Considering a triangular function along the y-direction with its top corresponding to the y-center of this image and its base going from the y-center of the previous image to the y-center of the next image, we compute an array

of “ramp coefficient” per oversampled detector pixel (called  $C_y$ ) corresponding to the integral of the triangular function between each pixel boundaries.

- The trace computation provides, for each detector pixel, its wavelength boundaries and the corresponding average wavelength. Those are used to modulate the matrix  $C_y$  with the average throughput within the pixel computed from the attached vector and the detector throughput, and then converted from  $W/m^3$  into photons.
- The trace also provides the sub-pixel position of the x-center of the slice as a function of the vertical position on the detector. Using this information, we assign coefficients per detector row to spread the flux over the detector pixels (matrix  $C_x$ ).
- The two matrices  $C_x$  and  $C_y$  are multiplied to form, the matrix  $C$  as shown on the Figure 3.
- The monochromatic image is resampled to the same grid as the oversampled detector map and convolved with the matrix  $C$  to obtain the flux map associated with the image footprint on the detector, i.e., on the pixels in between the centers of the previous and following images as shown on the left side of Figure 4.
- The resulting image is then summed on the final detector array to obtain the total flux as shown on the right side of Figure 4.

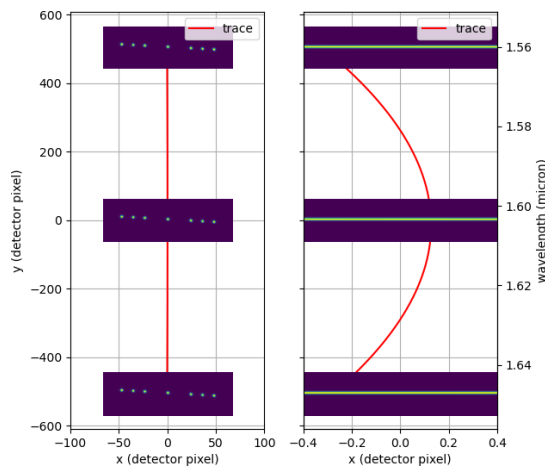


Figure 2. (Left) Three successive images from the image list and the associated trace shown as a red line. (Right) Zoomed-in view to highlight the distortion effect.

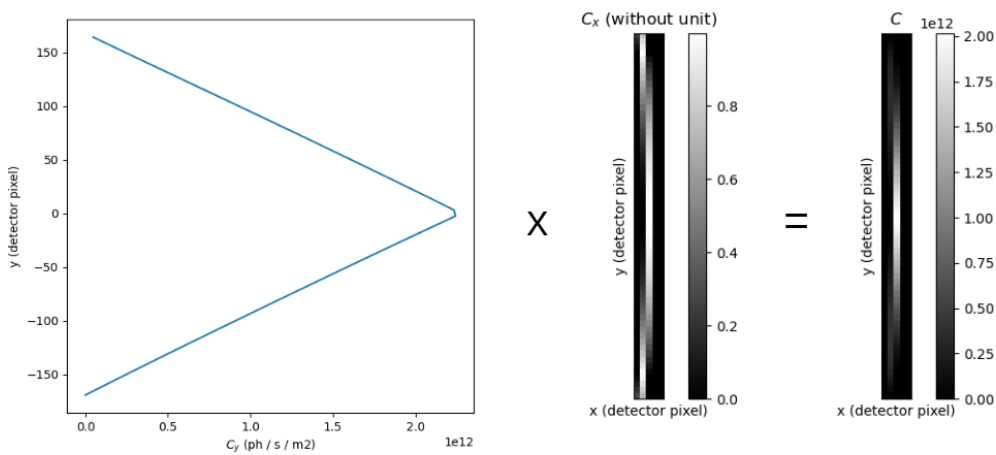


Figure 3. The matrix  $C$  used to expand the input image is the combination of a triangular function and the trace.

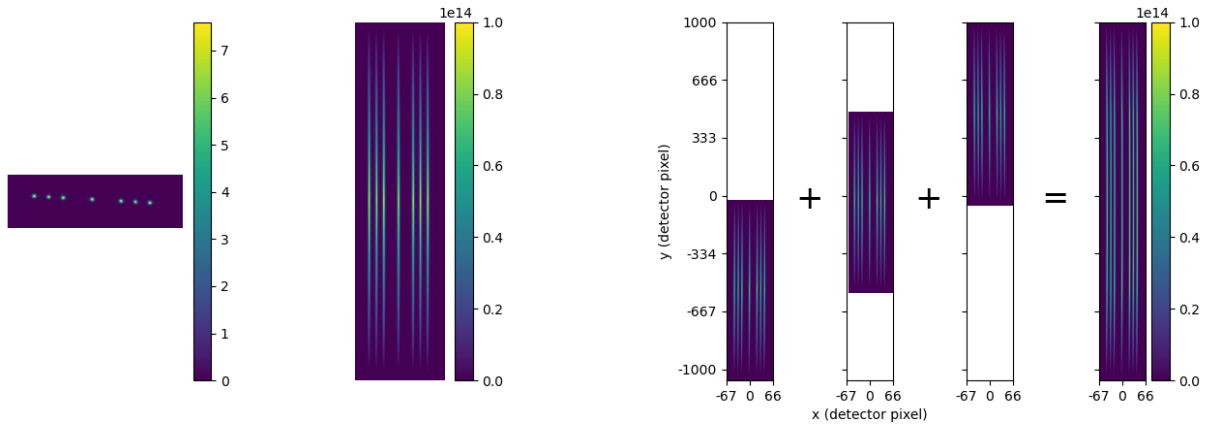


Figure 4. (Left) Input image and resulting image after convolution by the matrix C. (Right) The addition of the three images from Figure 2 after convolution by the matrix C gives the right-most image.

### Detector modeling

Once all the images are propagated and summed, the resulting oversampled map is then re-binned to match the detector pixel size. HARMONI operates across both the visible and near-infrared spectra, using four  $4k \times 4k$  CCDs for visible wavelengths and eight  $4k \times 4k$  HgCdTe detectors for the near-infrared wavelengths, each with 15 micrometers square pixels. In both cases, the simulation of the detectors is divided into two parts.

The chromatic part is simulated with the light propagation through the instrument, and corresponds to the photon to electron conversion. It produces as output an electron rate map, representing the number of electrons per second reaching each detector pixel. Effects modeled in the chromatic part of the simulation include the sampling by the detector matrix, quantum efficiency and charge diffusion.

The non-chromatic part simulates the detector read-out process to convert the electron rate maps into read-out frames, which can be a simple frame for the visible detectors, or multiple sample-of-the-ramp frames for the near-infrared detectors. The simulated effects include dark current, hot and dark pixels, cosmic rays, cross-talk, non-linearity, different type of read-out noise and conversion into ADU. The near-infrared simulation is based on the JWST/NIRSpec simulator developed at CRAL [10] and on the HxRG Noise Generator (NG) [11].

The separation of the simulation in two parts and the coupling to the light propagation is needed to avoid storing vast amount of data in the chromatic part (one value per pixel and per wavelength). It also decouples as much as possible the modeling of the detector and the observation parameters from the instrument modeling itself, and enables the possibility to run the non-chromatic part from an existing electron-rate map without running the full simulation. In addition, the electron-rate maps have proven valuable as an interesting intermediate output for the data reduction pipeline algorithm development due to their noiseless nature.

The final output is saved as a FITS file containing the data for either the eight near-infrared detector or the four visible detectors of HARMONI, along with adequate headers describing observing parameters, just as the real instrument will do. The left side of Figure 5 presents the resulting detector image of the path H for Antennae Galaxies simulation, while the right side displays the detector image of the path A for the trace mask calibration simulation.

We are currently exploring the integration of the Pyxel framework [12] into our simulator. This Python-based software is capable of simulating various types of imaging detectors and has been developed in order to avoid re-developing and re-implementing simulation codes, models and tools for every new instrument and share simulation models. For HARMONI, this framework would enable the simulation of additional detector effects, such as persistence which can significantly impact the operational scheduling of the instrument. In addition, the “model calibration” mode of Pyxel shows potential for creating detector models from data that will be acquired as part of the detector characterization process.

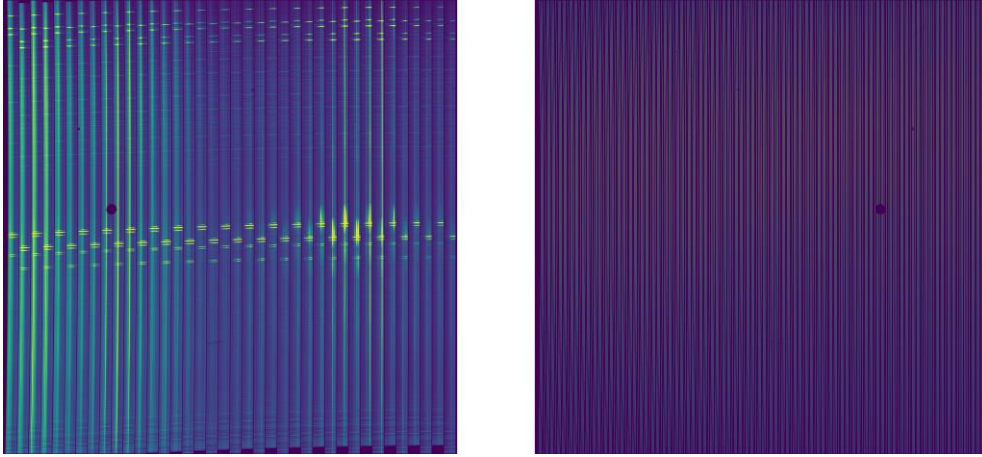


Figure 5. (Left) Resulting detector image of the path H for Antennae Galaxies simulation presented on Figure 1. (Right) Resulting detector image of the path A for the trace mask calibration simulation presented on Figure 1.

### Simulating part of the ESO Data Flow System (DFS)

Observations at all ESO telescopes are carried out by executing Observation Blocks (OBs) provided by the users. An OB consists in a list of templates which come in different types: acquisition templates, science templates, attached calibration template, daily calibration templates and technical templates.

HINM uses a configuration file modeled after the OB system to define the sequence of exposures to simulate. It contains the list of templates to execute and their parameters specifying for each exposure the telescope pointing and the instrument settings (AO mode, scale, grating, position of mask wheels, etc.). Simulating an on-sky observation also requires defining the astronomical target and numerous observation parameters and conditions (ambient conditions, seeing, date, etc.), while simulating calibration exposures needs descriptions of masks and lamps used.

From this configuration file, exposures are simulated sequentially, adding the exposure time and sky offsets to calculate the start date and time and sky location of the next exposure. For each exposure, a single FITS file with the same format as the real instrument will produce is created. Each detector data is stored in a different image extension and the FITS header contains all metadata required by ESO standards [13]. In particular, ESO hierarchical keywords collect information such as data category and purpose of the data, parameters related to the parent observation block and template, observing date and conditions, telescope setup and pointing, instrument settings (adaptive optics system, rotator, optical elements configuration, detector parameters), and most information from the different subsystems.

### Gathering data to build the HINM database

HINM integrates a database that characterizes all simulated effects for every mode and configuration of the instrument. This database, approximately 4 GiB in size, includes detailed information on optical parameters of the instrument modules and elements, coordinate transforms between the key optical planes, wave-front error maps, transmission curves (mirrors reflectivity curves, filter transmissions, the disperser efficiencies, etc.), detectors parameters.

Populating this database is a significant work, requiring the collection of data from various HARMONI systems. A significant portion of the data is directly extracted from the optical design of the instrument. The software used within the consortium to design the instrument optics is Ansys Zemax OpticStudio. Custom scripts based on the ZOS-API expanding this software have therefore been developed to extract the required information. Transmission curves typically come from system specifications, which are often determined through measurements of samples or engineering devices. The reflectivity curves for the ELT mirrors are provided by ESO.

The database is continuously updated to align with the evolving design of the instrument. It will be updated with measurements as the first components are manufactured. That way the HINM software will closely replicate the HARMONI instrument, making it a digital twin from the optical point of view.

### 3. HINM USAGES

The HINM software is not an ESO deliverable, but its products are ESO deliverables. It is used extensively to develop and prototype the data reduction pipeline [14], which performs the inverse process, producing a 3D data cube from the raw detector data. This section shows a few examples, ranging from technical to scientific applications.

#### **Testing the data reduction workflow with HINM simulated data**

The HARMONI data reduction pipeline is designed following the ESO standards and consists of a series of standalone programs known “recipes”. Each recipe is designed to process certain types of input data, such as science exposures and the associated calibration exposures. Although users can run the recipes independently, within the ESO DFS, the selection of the appropriate input data for the different recipes, and their execution in sequence are scheduled automatically to create the final science data products. The framework for running ESO data processing pipelines is currently being upgraded to the ESO Data Processing System (EDPS) [15].

Therefore, we need to test the compatibility of the HARMONI data reduction pipeline with EDPS. As the data reduction cascade depends on the FITS headers keywords of the data to process (instrument configuration, template used, sky subtraction strategy, etc.), data classification and files associations can be complex. The compliance check requires simulating data that contains all mandatory keywords. HINM has been used to generate sets of raw data that simulate both science exposures and calibration exposures. Then, for each dataset, EDPS has been instructed to generate the corresponding final science data product.

#### **Prototyping the geometrical calibration**

We used HINM to develop and test the algorithm for the geometric calibration, a key step in the data reduction process. This algorithm determines the coordinate transforms from detector pixels to wavelength and relative spatial position in the telescope focal plane. The diversity of configurations in the HARMONI instrument, and the stringent accuracy requirements required the development of a challenging algorithm minimizing the number of calibration exposures per configuration and keeping the calibration time acceptable. The paper [16] provides a mathematical description of the algorithms involved in the geometrical calibration and presents validations on mock data created with our simulator. The simulated calibration exposures presented in the paper are performed using the masks of the calibration module, located outside the instrument cryostat. However, a first analysis on instrument stability revealed that the pre-optics masks located within the cryostat should be used to refine the previous analysis done with masks from the calibration module. Additionally, the HARMONI instrument acquisition sequence has been updated for a more accurate pointing. Consequently, we plan to update our simulator to include the pre-optics masks and the pointing model, which will help us redesign and validate the geometrical calibration algorithm.

#### **Building a database of calibration products for periodic integration**

As part of the pipeline development, we periodically generate consistent set of exposures with HINM for both daily calibration and on-sky exposures, and for every mode and configuration of HARMONI. This results in several terabytes of raw data. The pipeline then ingests this raw data to produce calibration products, which include quality control (QC) headers. These headers are checked to ensure the data reduction process operates correctly and with the required accuracy. Once validated, the corresponding calibration products are stored and can be reused to reduce science simulations.

#### **Science simulation: Antennae Galaxies**

Our simulator was also used to simulate some typical HARMONI science cases, such as the Antennae Galaxies (NGC 4038/39) redshifted to  $z=2$ . This astrophysical scene was created from a VLT/MUSE observation [17]. In order to optimize the simulation time, the original data cube was divided into a continuum cube with low spectral resolution and eight smaller cubes centered around the emission lines with higher spectral resolution. The simulation was performed with the LTAO mode of HARMONI, the H+K grating and conducted for every spatial scale. Each observation took approximately 12 hours to simulate. These simulations allowed us to successfully test our data reduction pipeline prototype on multiple

scales, and various position angles. The resulting reduced data cubes were analyzed around the emission lines to validate the wavelength calibration process. Figure 6 shows a color image of the 60 mas scale simulation, generated by extracting the [SII], H $\alpha$ , [OIII] emission lines from the reduced data-cube and mapping them to the RGB channels.

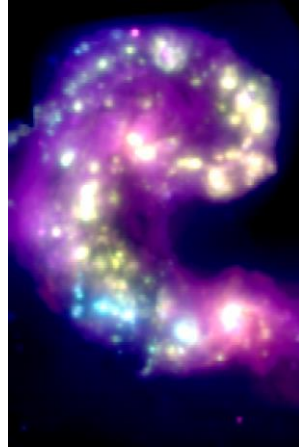


Figure 6. Color image of the Antennae Galaxies in 60 mas with grating H+K. The RGB channels maps to the [SII], H $\alpha$ , [OIII] emission lines.

### Science simulation: Io

Another science case for HARMONI is the observation of solar system bodies. Here we present an observation of Io, one of Jupiter's largest moons, simulated at the 4 mas scale using the H+K grating. The observation is made of eight exposures with different pointings, and allowed us testing the mosaicking feature and the correction of the differential atmospheric refraction of the data reduction pipeline prototype. Figure 7 shows the reduced white light image, but the full reduced data cube was also produced and offers the possibility to study Io's surface and obtain spectra of hot spots and volcanoes.

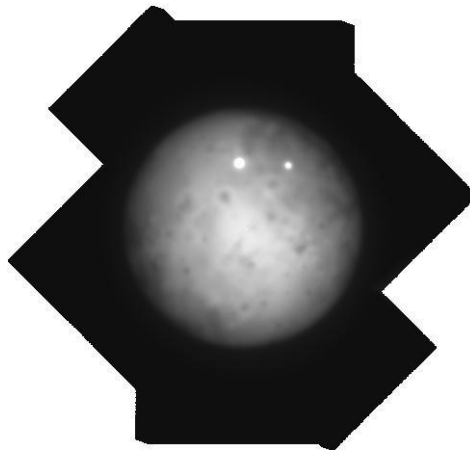


Figure 7. Reduced white light image of Io, obtained from eight exposures at the 4 mas scale with H+K grating.

### ACKNOWLEDGEMENTS

We thank Peter Weilbacher for sharing the reduced data of the Antennae Galaxy. We are grateful to Olivier Groussin for sharing the HSIM scene of Io. We acknowledge financial support from the Commission Spécialisée Astronomie Astrophysique (CSAA) of CNRS / INSU, as well as the Labex-LIO (Lyon Institute of Origins) under Grant No. ANR-10-LABX-66 (Agence Nationale pour la Recherche). We gratefully acknowledge support from the PSMN (Pôle Scientifique de Modélisation Numérique) of the ENS de Lyon for the computing resources.

## REFERENCES

- [1] Thatte, N., et al, “HARMONI: the ELT's First-Light Near-infrared and Visible Integral Field Spectrograph”, *The Messenger*, vol. 182 (2021). <https://doi.org/10.18727/0722-6691/5215>
- [2] Zieleniewski, S., et al., “HSIM: a simulation pipeline for the HARMONI integral field spectrograph on the European ELT”, *MNRAS*, vol. 453 (2015). <https://doi.org/10.1093/mnras/stv1860>
- [3] Goodman, J. W., “Introduction to Fourier Optics”, McGraw-Hill, Columbus, OH, 2nd ed. (1996).
- [4] Denis, L., et al., “Fast approximations of shift-variant blur”, *International Journal of Computer Vision*, Springer Verlag, vol. 115 (2015). <https://doi.org/10.1007/s11263-015-0817-x>
- [5] Schwartz, N, et al., “Preparation of AO-related observations and post-processing recipes for E-ELT HARMONI-SCAO”, *Proc. SPIE*, vol. 9909 (2016). <https://doi.org/10.1117/12.2231291>
- [6] Neichel, B. et al., “TIPTOP: a new tool to efficiently predict your favorite AO PSF”, *Proc. SPIE*, vol. 11448 (2020). <https://doi.org/10.1117/12.2561533>
- [7] Noll, S., et al., “An atmospheric radiation model for Cerro Paranal. I. The optical spectral range”, *A&A*, vol. 543 (2012). <https://doi.org/10.1051/0004-6361/201219040>
- [8] Jones, A., et al., “An advanced scattered moonlight model for Cerro Paranal”, *A&A*, vol. 560 (2013). <https://doi.org/10.1051/0004-6361/201322433>
- [9] Filippenko, A. V., “The importance of atmospheric differential refraction in spectrophotometry.”, *PASP*, vol. 94 (1982). <https://doi.org/10.1086/131052>
- [10] Piqueras, L., et al., “The JWST/NIRSpec instrument performance simulator software”, *Proc. SPIE*, vol. 7738 (2010). <https://doi.org/10.1117/12.856860>
- [11] Rauscher, B. J., “Teledyne H1RG, H2RG, and H4RG Noise Generator”, *PASP*, vol. 127 (2015). <https://doi.org/10.1086/684082>
- [12] Arko, M., et al., “Pyxel 1.0: an open source Python framework for detector and end-to-end instrument simulation”, *JATIS*, vol. 8 (2022). <https://doi.org/10.1117/1.JATIS.8.4.048002>
- [13] Dobrzycki, A., “ESO Data Interface Control Document”, ESO-044156.
- [14] Piqueras, L., et al., “Preliminary design of the HARMONI science software”, *Proc. SPIE*, vol. 9911 (2016). <https://doi.org/10.1117/12.2232440>
- [15] Freudling, W., et al., “Adaptive data reduction workflows for astronomy: The ESO Data Processing System (EDPS)”, *A&A*, vol. 681 (2024). <https://doi.org/10.1051/0004-6361/202347651>
- [16] Piqueras, L., et al., “HARMONI first light spectroscopy for the ELT: geometrical calibration in the data reduction software”, *Proc. SPIE*, vol. 11452 (2020). <https://doi.org/10.1117/12.2560485>
- [17] Weilbacher, P. M., et al., “Lyman-continuum leakage as dominant source of diffuse ionized gas in the Antennae galaxy”, *A&A*, vol. 611 (2018). <https://doi.org/10.1051/0004-6361/201731669>